Computational Challenges in Nuclear and Many-Body Physics
Stockholm, September 15th – October 10th

Combined ab initio-mean field approach to solute-atom diffusion in alloys

Luca Messina[a], Pär Olsson[a], Maylise Nastar[b]

In collaboration with: Thomas Garnier[b]
Christophe Domain[c]

October 7th 2014
NORDITA, Stockholm

[a] Reactor Phisics, KTH, Stockholm [b] SRMP, CEA Saclay, Paris [d] MMC, EDF Les Renardières, Paris

Outline

1. Solute diffusion and applications
2. Onsager matrix (transport coefficients)
3. First-principles calculations of jump rates
4. Self-consistent mean field model
5. Application to bcc Fe-X model dilute alloys
6. Radiation-induced segregation
7. Conclusions

Solute diffusion in alloys

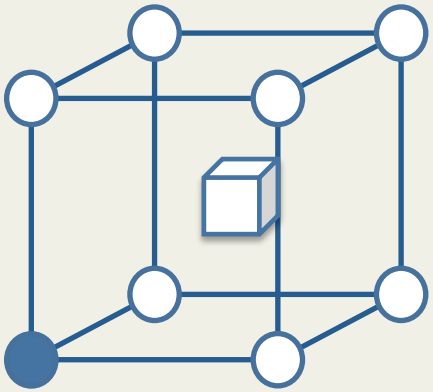

Vacancy exchange

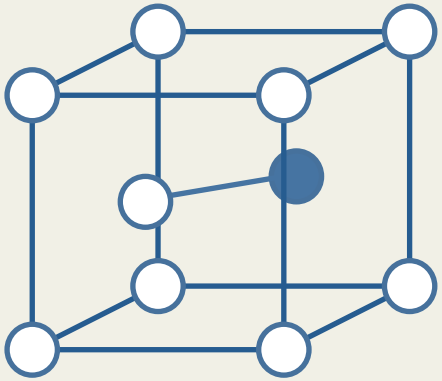

Dumbbell migration

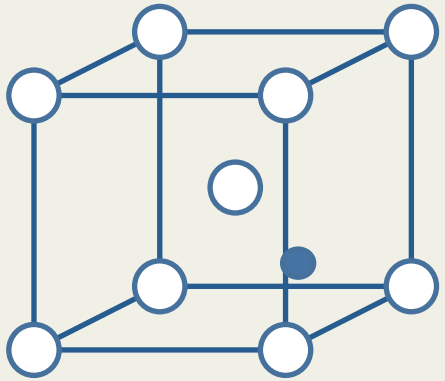

Foreign interstitial

Diffusion capability depends on:

- Stability of the defected configuration (binding energies).
- Transition (jump) rates.

$$P_{config} \propto \exp\left(\frac{-E^{B}_{config}}{k_B T}\right) \qquad \omega = \nu \exp\left(-\frac{E^{M}}{k_B T}\right)$$

Solute diffusion in alloys

INVERSE KIRKENDALL MECHANISM

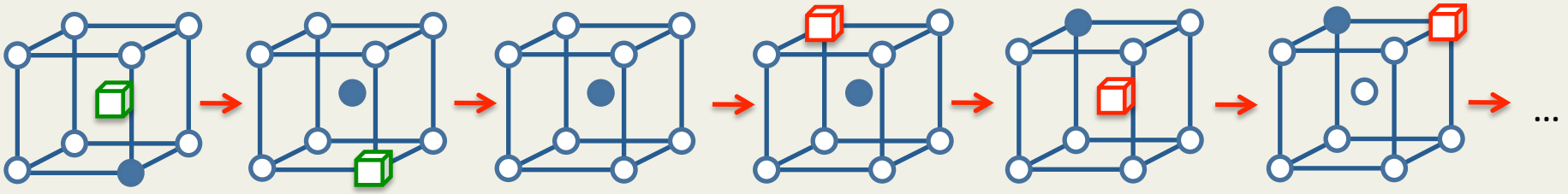

VACANCY DRAG

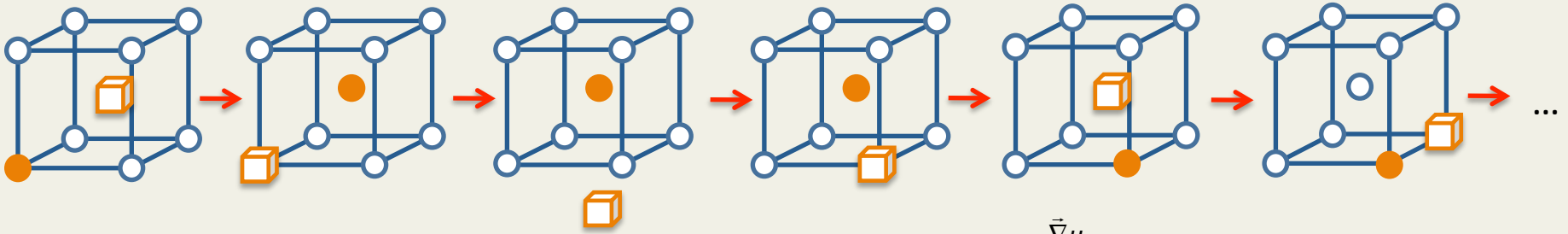

$\vec{\nabla}\mu_x$

Defect chemical potential gradient

DUMBBELL MECHANISM (rotation-translation)

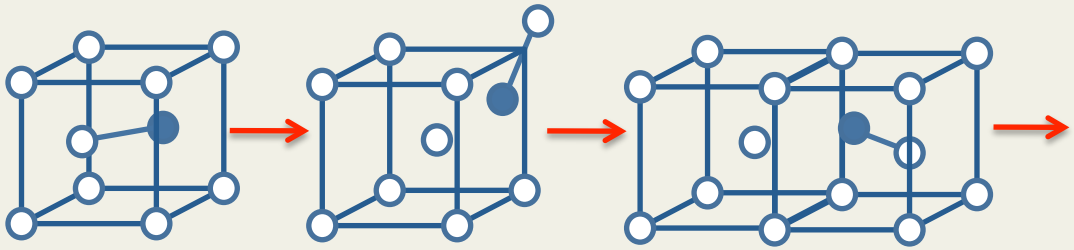

Experimental difficulties due to:
- Slow diffusion processes at low temperatures.
- No extrapolation from high T in magnetically-ordered systems.
- Resolution of material analysis techniques.

Microstructural characterization

Diffusion mechanisms are important to control many **metallurgical processes** requiring a very precise microstructural characterization.
Examples [1,2] :
- Ad-hoc heat treatments to induce phase separation.
- Enhancement of mechanical properties through formation of hardening phases.

Diffusion mechanisms are also responsible for **degradation of mechanical properties**!
Example: Embrittlement of Reactor Pressure Vessel (RPV) steels in nuclear reactors.

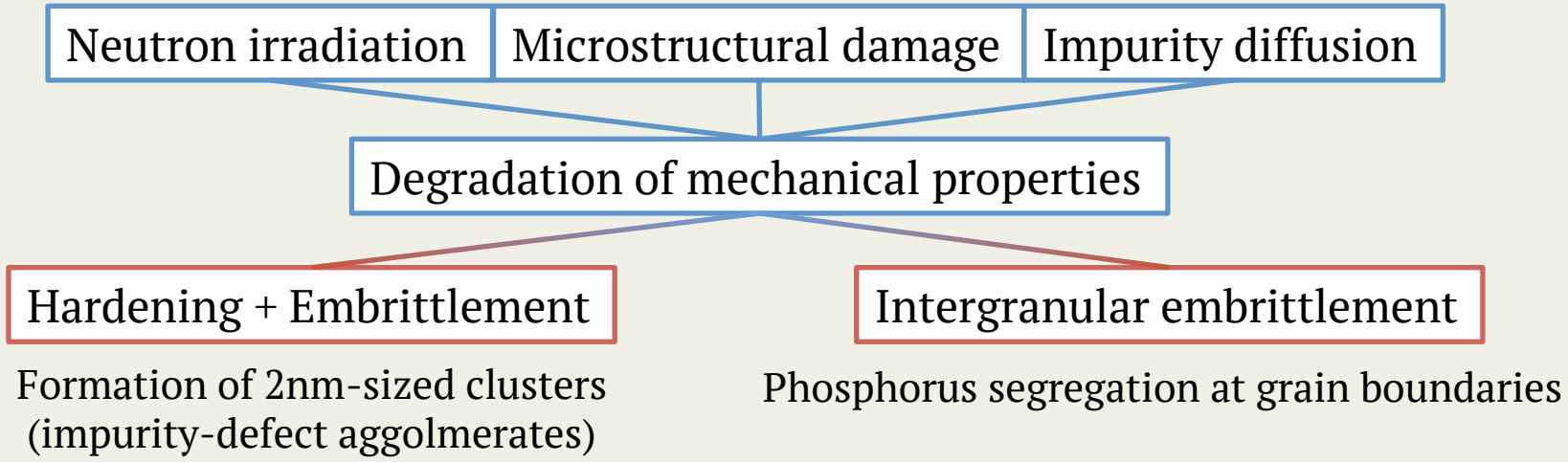

[1] Z. Mao et al., Nat. Mater. 6, 210 (2007).
[2] F. Danoix et al., Adv. Eng. Mater. 8, 1202 (2006).

Embrittlement in RPV steels

Atom maps (R4)

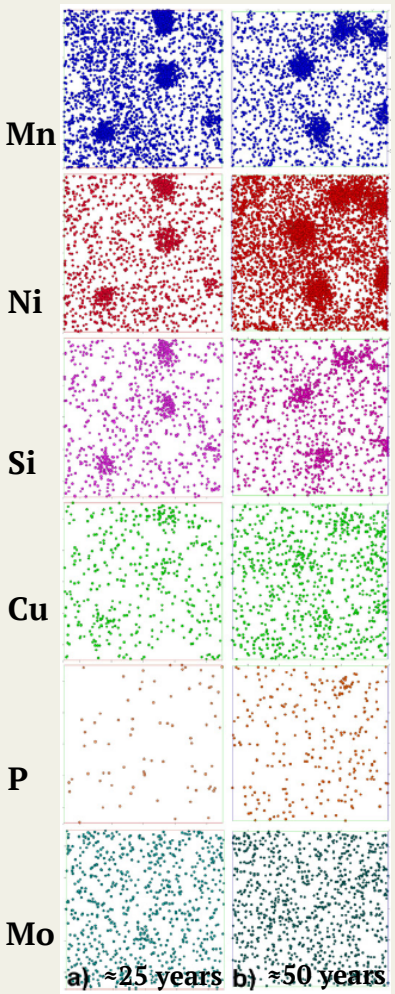

Mn-Ni-(Si)-(Cu) nanocluster (R3)

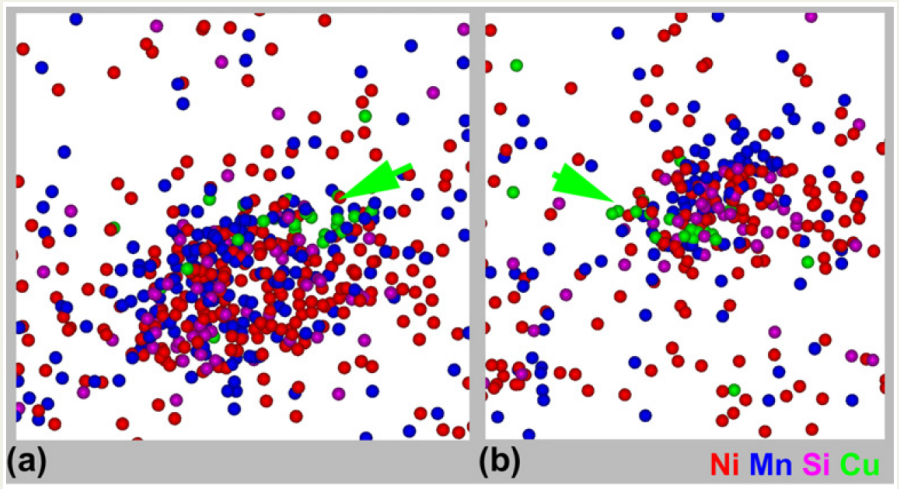

P segregation to dislocations (R4)

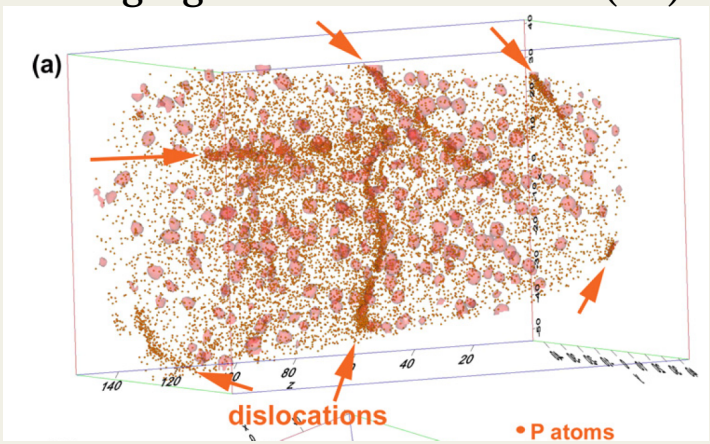

Miller et al., JNM 437 (2013)

Ringhals surveillance capsules (atom probe tomography)

Mn-Ni-Si rich precipitates

(radiation-induced)

Cu-rich precipitates

(radiation-enhanced)

Onsager matrix

FICK'S LAW

$$J_i = -\sum_{j=1}^{N} D_{ij} \nabla C_j$$

ONSAGER'S FORMULATION [3]

$$J_i = -\sum_{j=1}^{N} L_{ij} \nabla \mu_j$$

- Off-diagonal coefficients (symmetric) describe flux correlations.

- Clear separation between thermodynamic and kinetic properties of the system.

$$J_A = -L_{AA}^{x} \nabla \mu_A - L_{AB}^{x} \nabla \mu_B$$

$$J_B = -L_{BA}^{x} \nabla \mu_A - L_{BB}^{x} \nabla \mu_B$$

FLUX COUPLING

Vacancy drag

Solute and vacancy flowing in the same direction.

$$\frac{-(L_{AB}^{V} + L_{BB}^{V})}{L_{BB}^{V}} > 0$$

Interstitial transport

Solute transported by dumbbells faster than solvent atoms.

$$L_{AB}^{I} + L_{BB}^{I} < L_{BB}^{I,0}$$

[3] A. R. Allnatt and A. B. Lidiard, *Atomic transport in solids* (Cambridge University Press, Cambridge, UK, 2003).

How to compute the L_{ij}'s?

EXPERIMENTS
- Low-temperature impediments.
- No off-diagonal coefficients.

KINETIC MONTE CARLO
- Good for benchmark!
- Difficult with trapping effects.

$$L_{ij} = \frac{\left\langle \Delta\vec{R}_i \cdot \Delta\vec{R}_j \right\rangle}{6V\tau}$$

MEAN FIELD
- Steady-state solution to **master equation**

$$\frac{dP(n)}{dt} = \sum_{n'} \left[W(n' \to n)P(n') - W(n \to n')P(n) \right] = 0$$

P(n) = probability of configuration n

$$P(n) \propto \exp\left(-\frac{E(n)}{k_B T} \right)$$

W(n'→n) = rate of transition between configuration n' and n

$$W(n' \to n) = \omega = \nu \exp\left(-\frac{E^M}{k_B T} \right)$$

- W depends on the **local chemical environment** around the moving defect!
- Need for interaction range cutoff.

Multifrequency network in dilute alloys

Vacancy, 2nn model

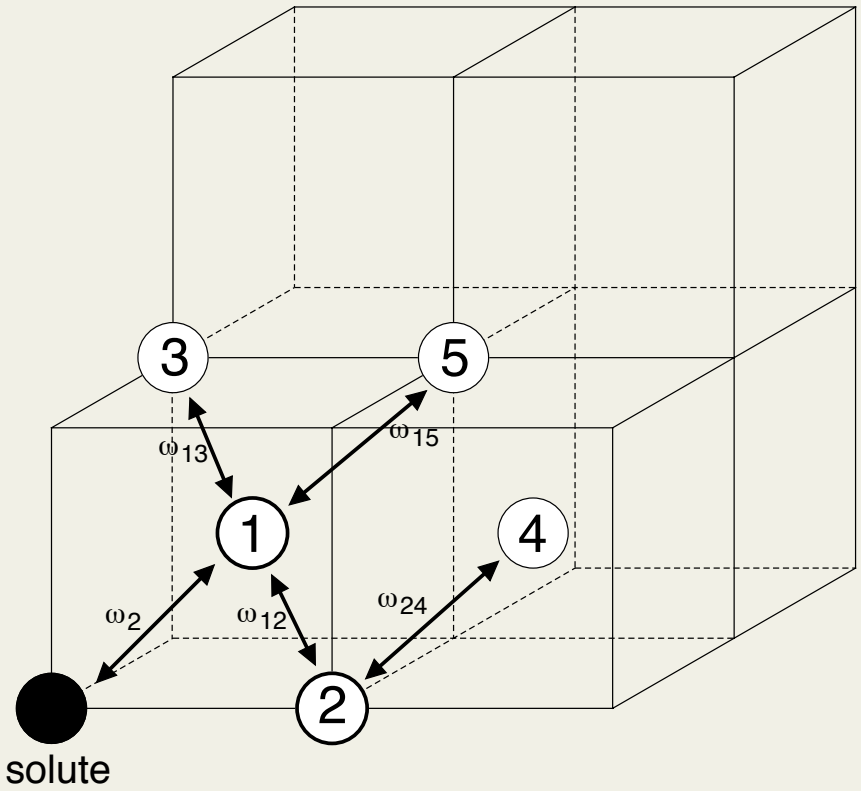

4+2 frequencies

Vacancy, 5nn model [4]

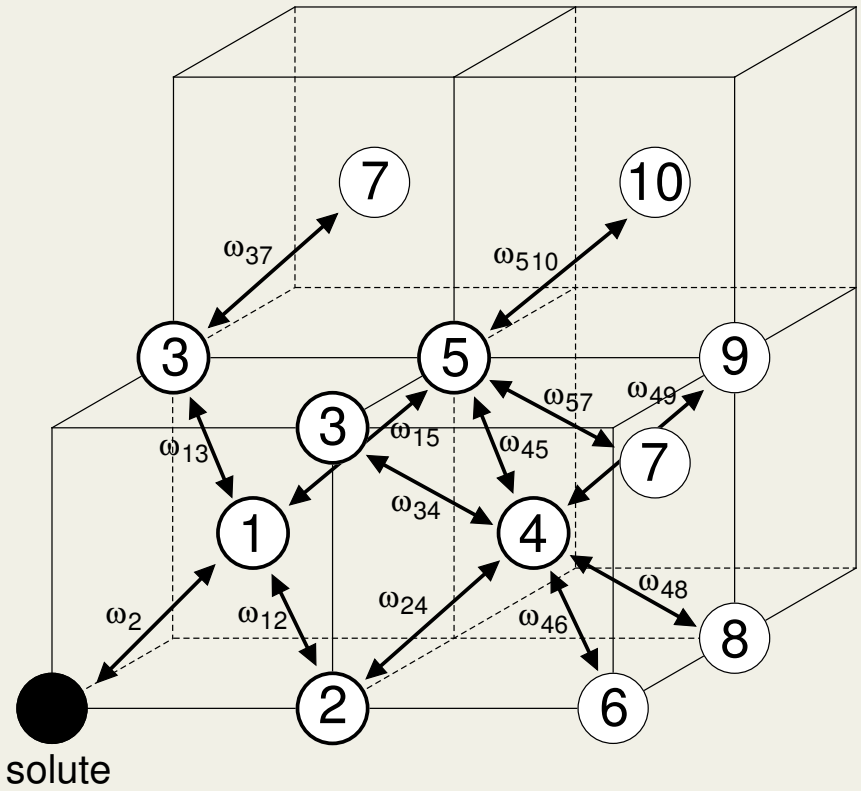

12+2 frequencies

[4] L. Messina *et al.*, PRB **90**, 104203 (2014).

Multifrequency network in dilute alloys

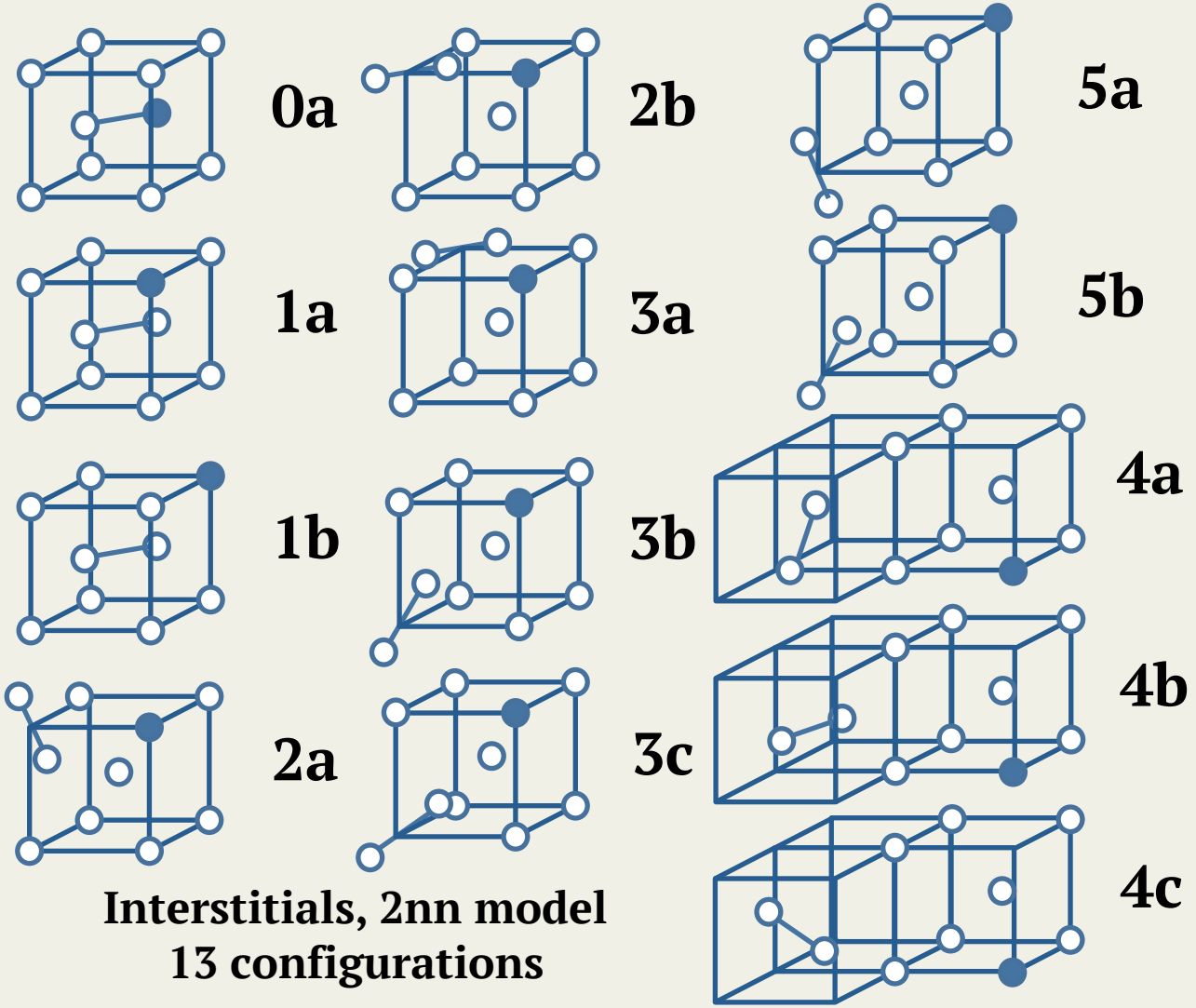

Interstitials, 2nn model
13 configurations

3 migration modes

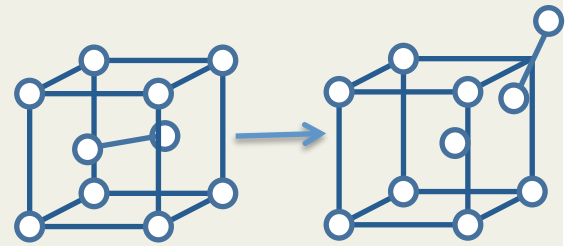

Rotation-translation (ω)

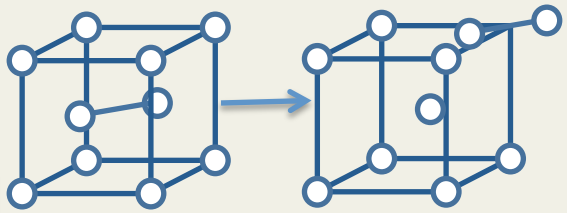

Translation (τ)

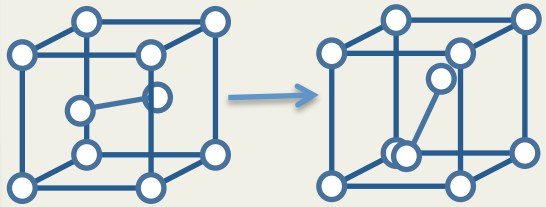

Onsite rotation (R)

Ab initio methodology

VASP SETTINGS
PAW-PBE method
Spin-polarized calculations
Full-core PAW potentials
Supercell: 128 atoms (vac), 250 atoms (int)
K-point mesh: 3x3x3
Cutoff energy: 300 eV (vac), 350 eV (int)
Refinement of mixing tags to prevent the simulation from getting trapped into a wrong magnetic state (Mn, Si).
Nudged Elastic Band (NEB) method
Phonon calculations (Hessian matrix)

BINDING ENERGIES

Supercell relaxation at constant volume.

ATTEMPT FREQUENCIES

(Vineyard's theory[9]):

$$\nu = \prod_{j=1}^{N-3} \nu_j^{init} \Big/ \prod_{j=1}^{N-4} \nu_j^{saddle}$$

MIGRATION BARRIERS (NEB)

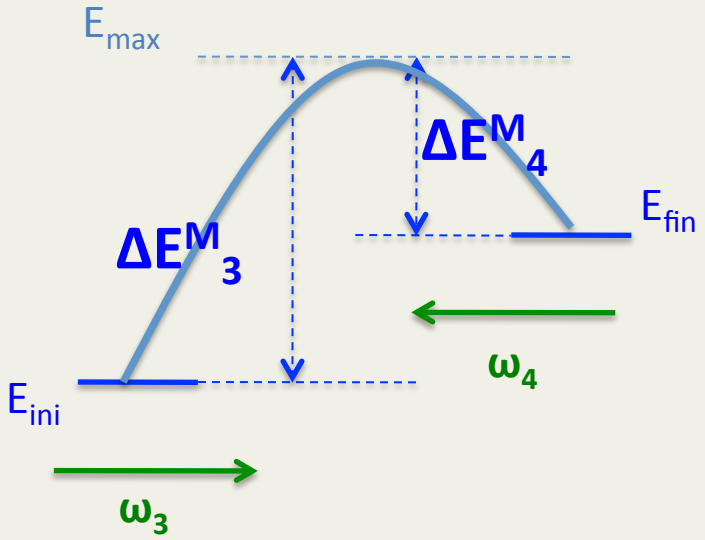

[9] G. H. Vineyard, J. Phys. Chem. Solids **3**, 121 (1957).

Ab initio results (V) [4]

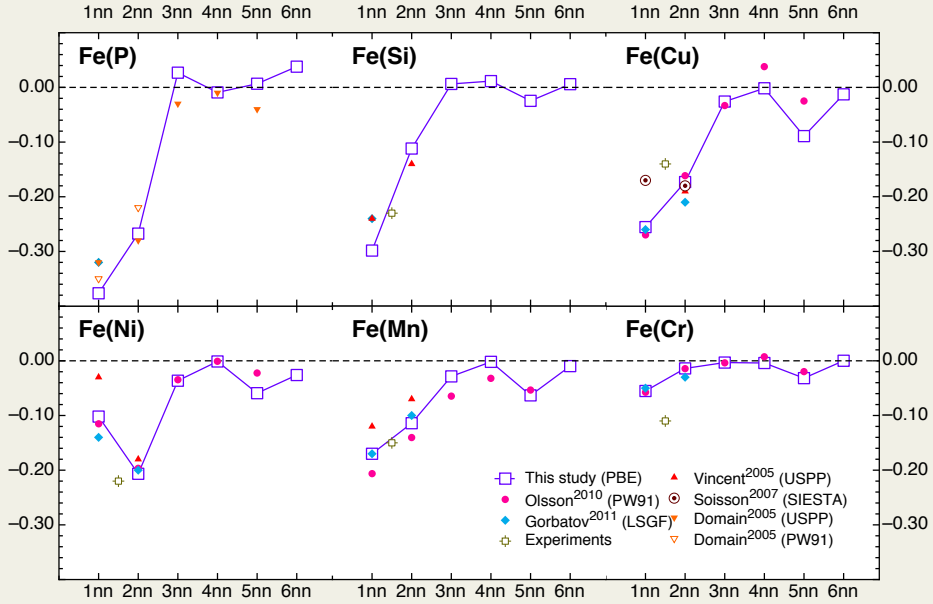

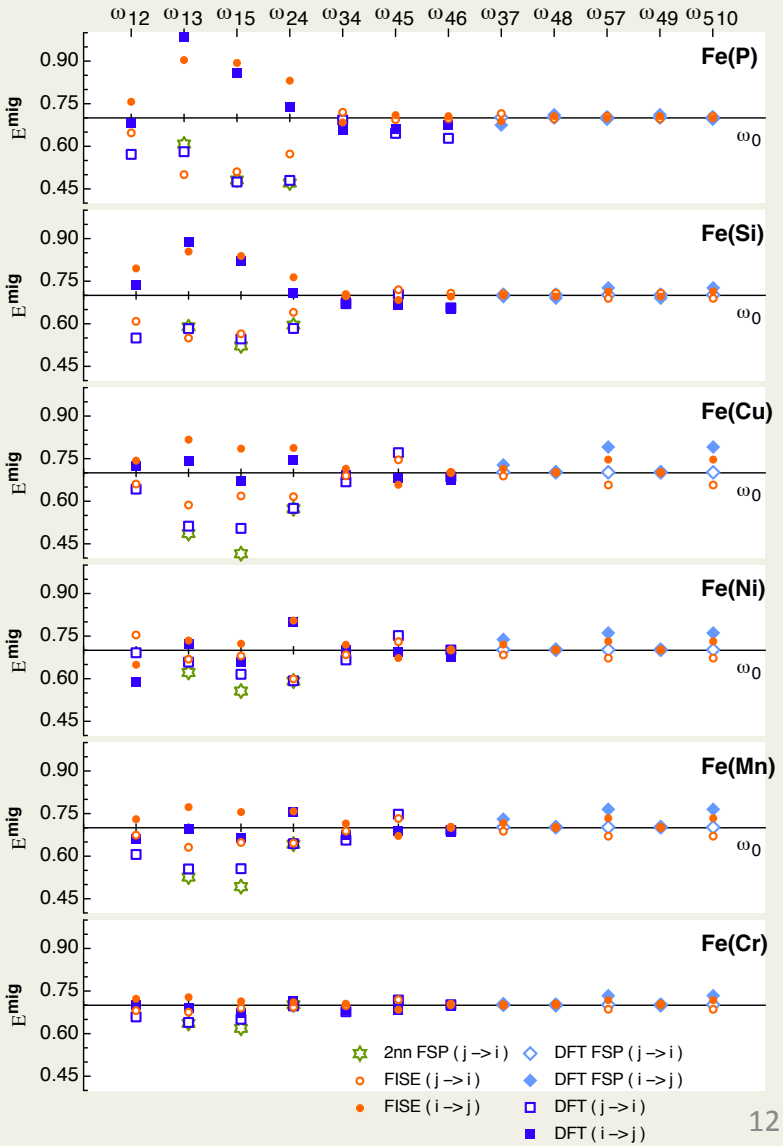

- Solute-vacancy interaction to 5nn.
- Migration barriers converging to background ω_0 with distance.

[4] L. Messina *et al.*, PRB **90**, 104203 (2014).

Ab initio results (I)

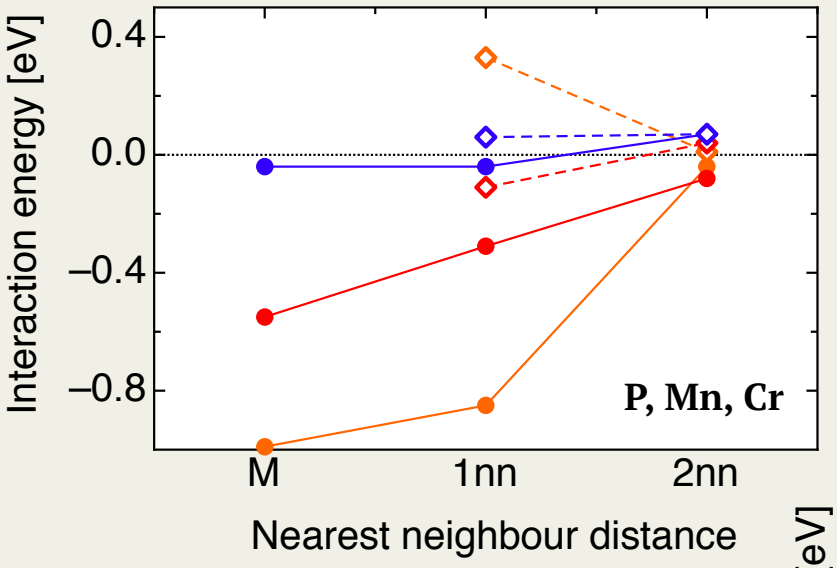

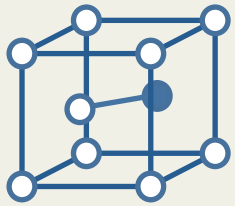

Mixed dumbbell (M)

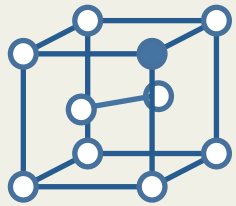

Tensile 1nn

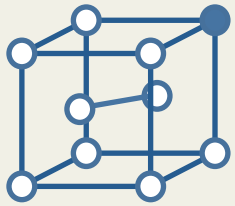

Compressed 1nn

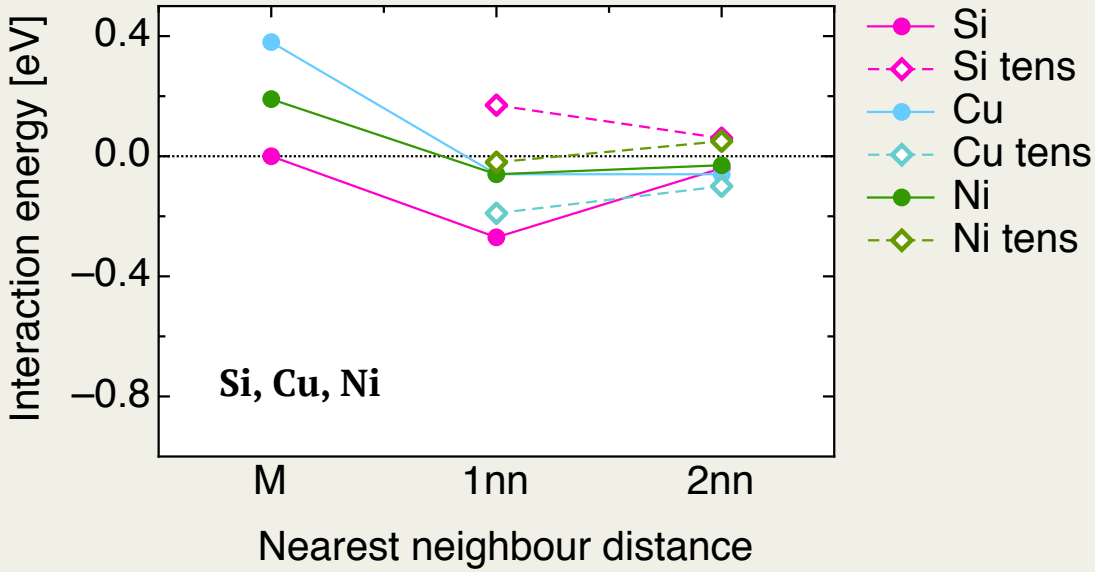

Ab initio results (I)

ω = Rotation–translation τ = Translation R = Onsite rotation

	0a	1a	1b	2a	2b	3b	3c	4b	4c	5b
0a	ω, τ, R		ω, τ							
1a		R	R	ω	ω, τ	ω, τ	ω			
1b	ω, τ	R	R	τ	ω	ω	τ			ω, τ
2a		ω	τ		R			τ	ω	
2b		ω, τ	ω	R	R			ω	ω, τ	
3b		ω, τ	ω							
3c		ω	τ							
4b				τ	ω					
4c				ω	ω, τ					
5b			ω, τ							

2nn model --> 27 + 3 frequencies (ω_0, τ_0, R_0 not shown)

Self-Consistent Mean Field method [5]

CONFIGURATION = ENSEMBLE OF OCCUPATION NUMBERS

$$n = \{n_1^A, n_1^B, \cdots n_1^v, n_2^A, n_2^B, \cdots, n_2^v, \cdots\}$$

$$n_i^\alpha = \begin{cases} 0 \\ 1 \end{cases}$$

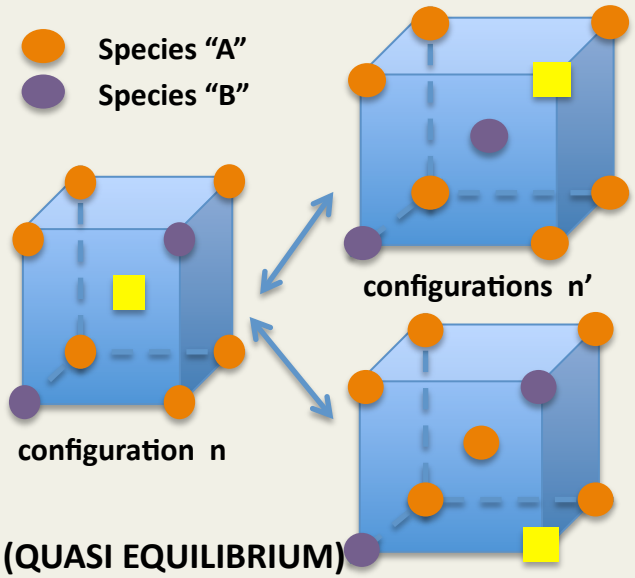

MASTER EQUATION

$$\frac{dP(n)}{dt} = \sum_{n'} [W(n' \to n)P(n') - W(n \to n')P(n)]$$

$$P(n) = P_0(n) \cdot P_1(n)$$

EQUILIBRIUM

The probability for a state to occur depends on the energy of the state according to the Boltzmann factor.

$$P_0(n) \propto \exp\left(-\frac{E_0(n)}{k_B T}\right)$$

$E_0(n)$: sum of pair interactions (possibly multi-body) THERMODYNAMIC INTERACTIONS

NON EQUILIBRIUM (QUASI EQUILIBRIUM)

Small perturbation from equilibrium state.
The variation of energy of the system is given by pair (possibly multi-body) interactions with the same mathematical structure.

KINETIC INTERACTIONS

$$P(n) \propto \exp\left(-\frac{E(n)}{k_B T}\right)$$

UNKNOWNS TO BE FOUND!

$$E(n) = \frac{1}{2!}\sum_{i \neq j, \alpha, \beta} n_i^\alpha n_j^\beta v_{ij}^{\alpha\beta} + \frac{1}{3!}\sum_{i \neq j \neq k, \alpha, \beta, \gamma} n_i^\alpha n_j^\beta n_k^\gamma v_{ijk}^{\alpha\beta\gamma} + \cdots$$

[5] M. Nastar, Philos. Mag. **85**, 3767 (2005).

Example 1: Vacancies

Example of kinetic interaction

1st : Configuration n can change when atom α jump from site i to a neighboring site s occupied by a vacancy.

2nd : Configuration n can change when atom β jump from site j to a neighboring site s occupied by a vacancy.

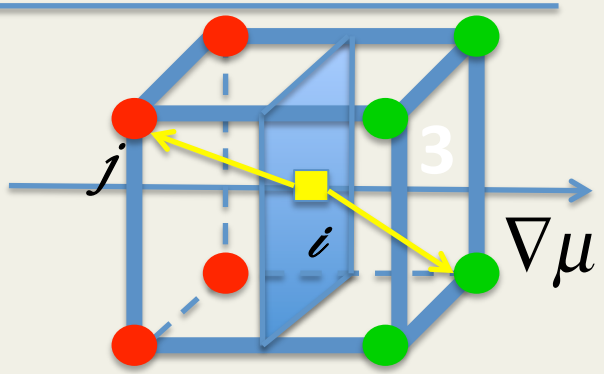

Symmetries: bond projection on $\nabla\mu$

$$\frac{d\left\langle n_i^{\nu} n_j^{\alpha}\right\rangle}{dt} = 0 = \beta \sum_{s\neq i\neq j,\sigma} \left\langle n_j{}^{\alpha} n_i{}^{\sigma} n_s^{\nu} \hat{\omega}_{is}^{\sigma\nu}\right\rangle^{(0)} \left(\mu_i^{\sigma} - \mu_s^{\sigma}\right) + \beta \left\langle n_i{}^{\alpha} n_j{}^{\nu} \hat{\omega}_{ji}^{\nu\alpha}\right\rangle^{(0)} \left(\mu_i^{\alpha} - \mu_j^{\alpha}\right)$$

$$+\beta \sum_{s\neq i\neq j,\sigma} \left[\sum_{k\neq s,\gamma} \left\langle n_j{}^{\alpha} n_i{}^{\sigma} n_s^{\nu} n_k^{\gamma} \hat{\omega}_{is}^{\sigma\nu}\right\rangle^{(0)} v_{sk}^{\sigma\gamma} - \sum_{k\neq i,\gamma} \left\langle n_j{}^{\alpha} n_i{}^{\sigma} n_s^{\nu} n_k^{\gamma} \hat{\omega}_{is}^{\sigma\nu}\right\rangle^{(0)} v_{ik}^{\sigma\gamma} \right] \quad \textbf{1st}$$

$$+\beta \left[\sum_{k\neq s,\gamma} \left\langle n_i{}^{\alpha} n_j{}^{\nu} n_k{}^{\gamma} \hat{\omega}_{ji}^{\nu\alpha}\right\rangle^{(0)} v_{jk}^{\alpha\gamma} - \sum_{k\neq s,\gamma} \left\langle n_i{}^{\alpha} n_j{}^{\nu} n_k{}^{\gamma} \hat{\omega}_{ji}^{\nu\alpha}\right\rangle^{(0)} v_{ik}^{\alpha\gamma} \right] \quad \textbf{2nd}$$

Example 2: Dumbbells

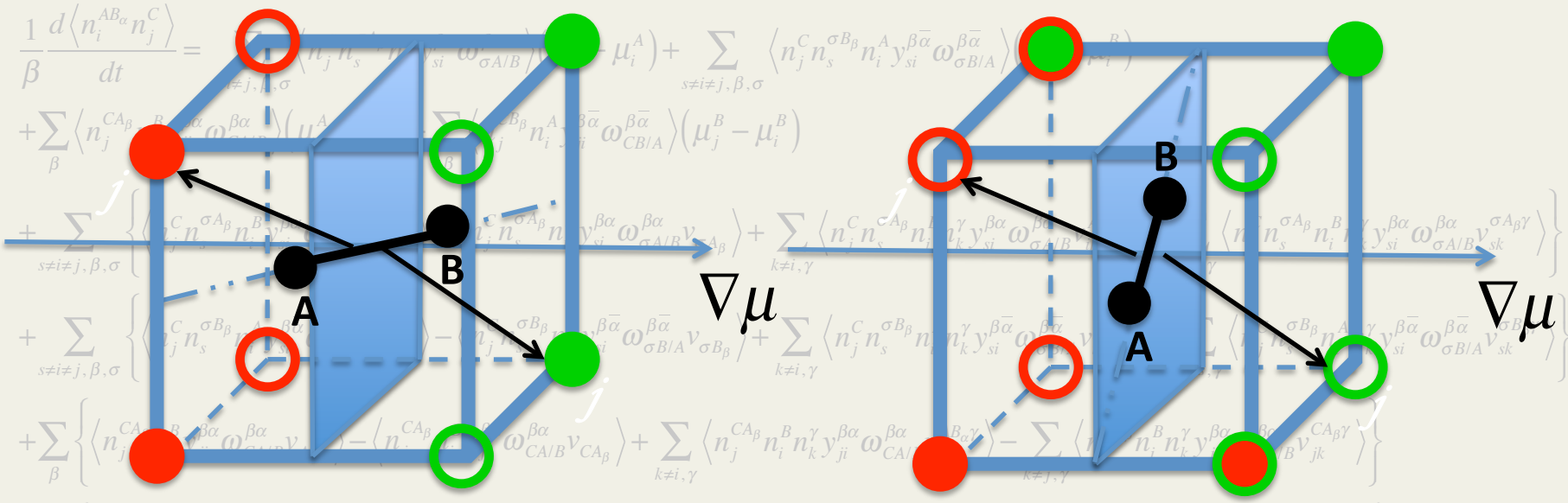

Solve system of equations:

$$\overline{T}\cdot\vec{V}_{ij}=\vec{b}(\nabla\mu_A,\nabla\mu_B)$$

Write down flux equations:

$$J^A_{i\to s}=-\beta l^{(0)}_A\left(\mu^A_s-\mu^A_i\right)-\beta\sum_{(\alpha,\beta,\sigma,\pi),\gamma}\left[l^{(1)}_A v_{\sigma A_\alpha}+l^{(2)}_A(\gamma)v^{\sigma A_\alpha\gamma}_{ik}\right]$$

$$\left(J_A=-L_{AA}\nabla\mu_A-L_{AB}\nabla\mu_B\right)$$

Automatic Matlab routines were developed at CEA[6] and KTH[7].

[6] T. Garnier *et al.*, PRB **88**, 134201 (2013).
[7] L. Messina *et al.*, to be submitted to PRB [2014].

Results: Vacancy drag [4]

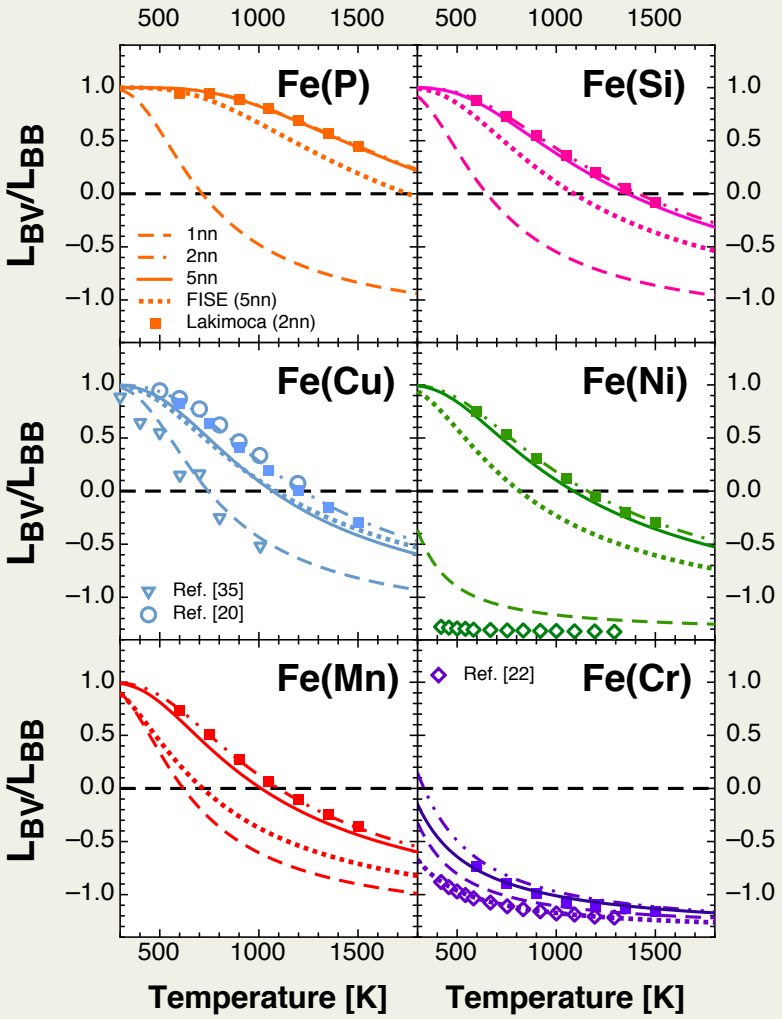

$$\frac{L_{BV}}{L_{BB}} > 0$$

- Vacancy drag occurring at low temperature for all solutes except Cr.
- Perfect benchmarking by KMC.
- Possibility of Ni, Si and Cu drag towards Mn-loop nuclei is confirmed.
- Contraddicting previous study in FeNi[8].
- Necessity of 2nn model in BCC.
- 5nn interaction negligible.

[8] S. Choudhury *et al.*, JNM **411**, 1 (2011).

[4] L. Messina *et al.*, PRB **90**, 104203 (2014).

Results: Solute diffusion coefficients

$$D_B^* = k_B T \frac{L_{BB}}{n c_B}$$

Comparison with previous multifrequency models

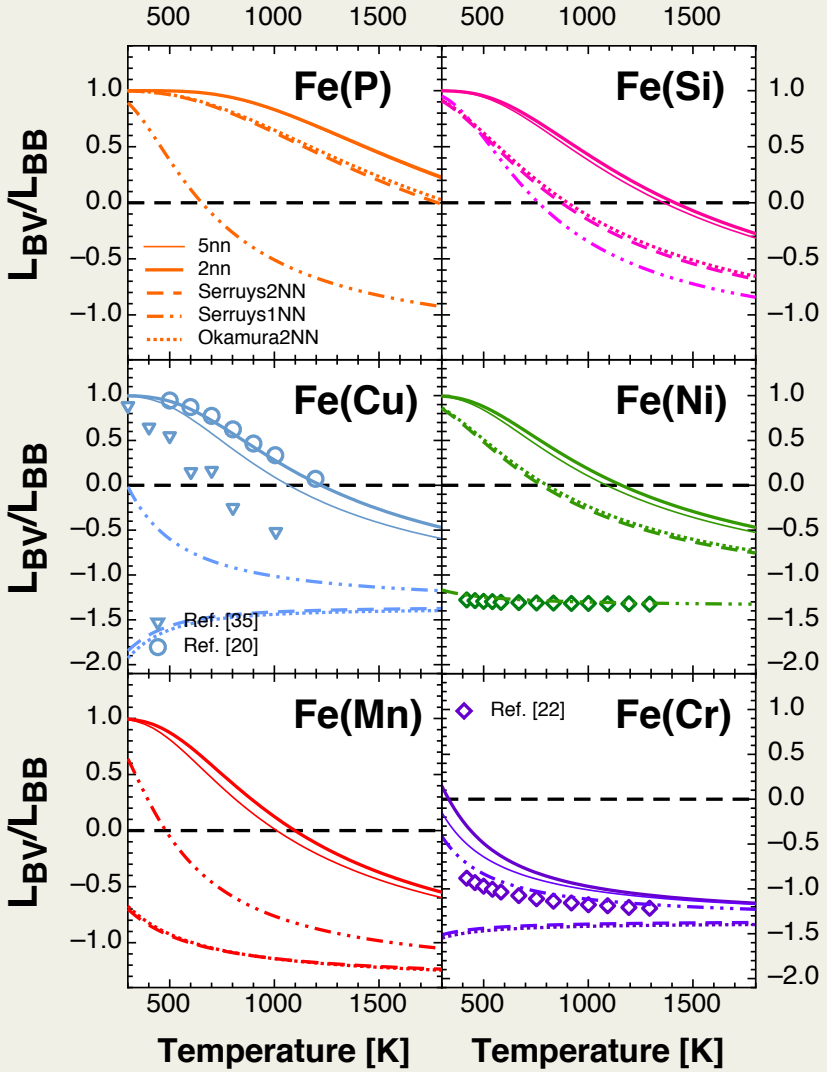

[4] Tracer diffusion coefficients D_B^*

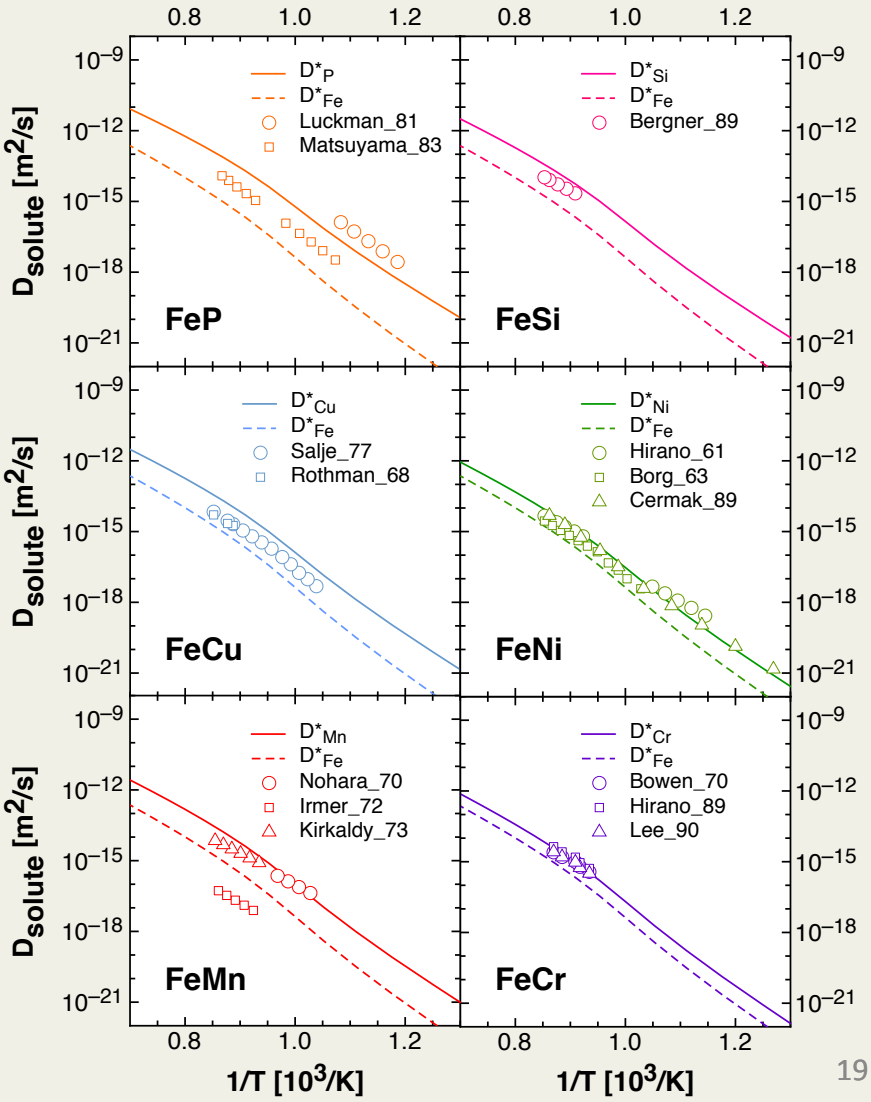

[4] L. Messina *et al.*, PRB **90**, 104203 (2014).

Results: Interstitial diffusion

Ratio of correlated to uncorrelated solute diffusion coefficient.

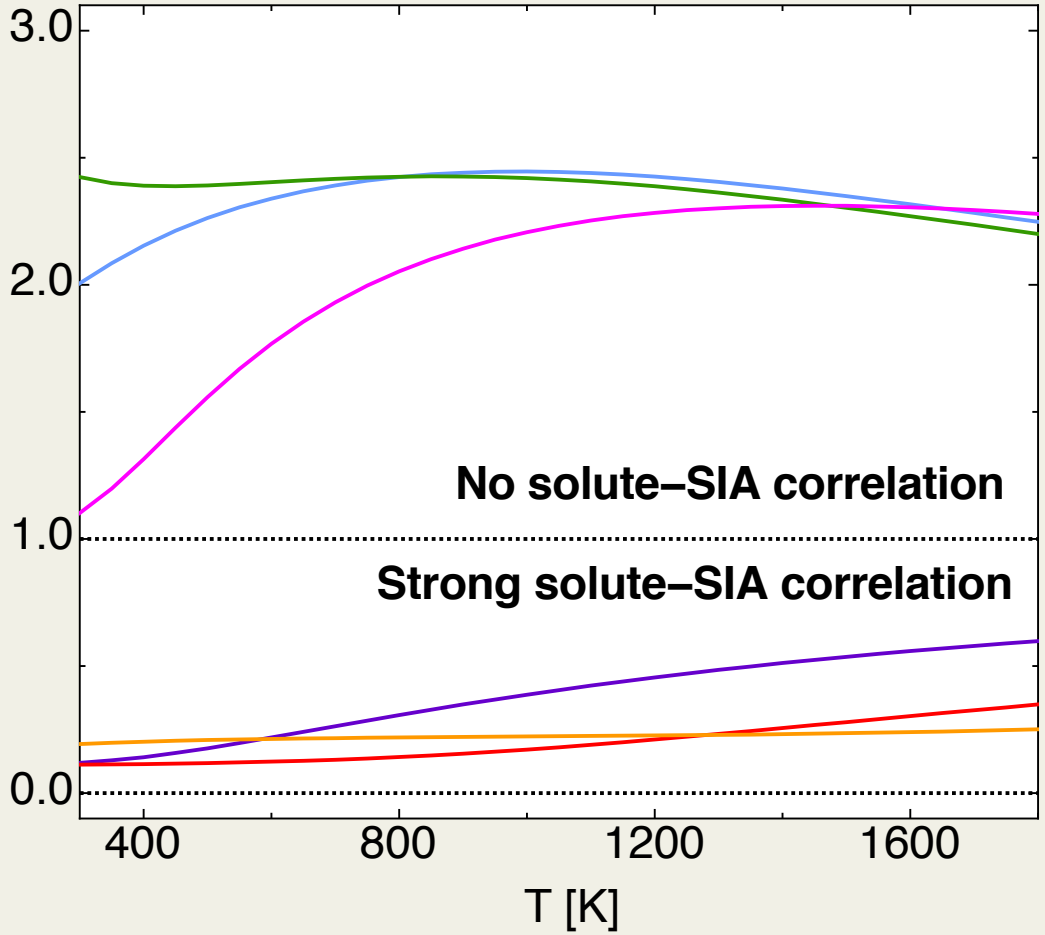

$$\frac{d_{BI}}{d_{BI}^{0}}$$

$$d_{BI} = \frac{L_{AB} + L_{BB}}{c_B c_I}$$ with correlations

$$d_{BI}^{0} = \frac{L_{BB}^{0}}{c_B c_I}$$ without correlations

Radiation-induced segregation (RIS)

Enrichment of solute atoms at defect sinks (grain boundaries, dislocations, precipitates).

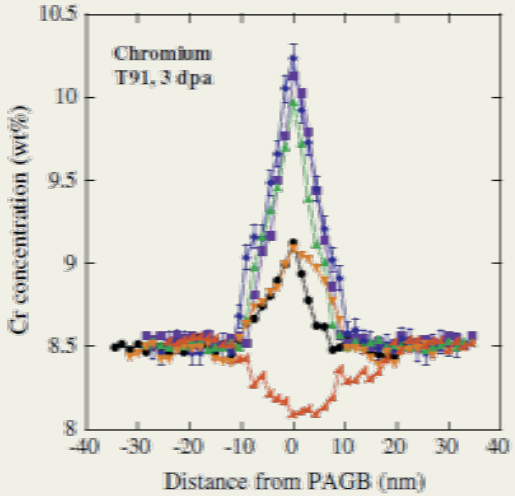

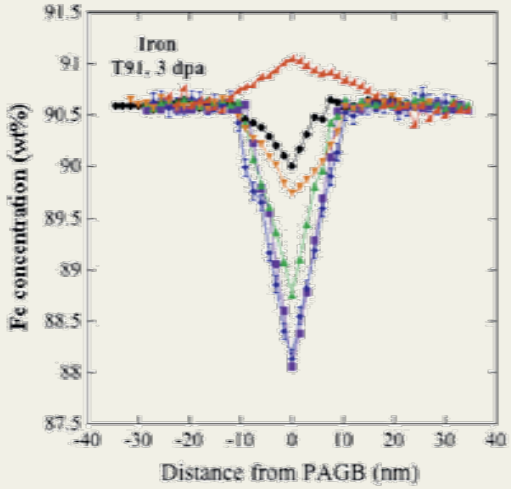

J.P. Wharry, G.S. Was, JNM 442 (2013)
Systematic experimental investigation of RIS in several F/M alloys at low temperature.

- Concentrated in Cr, dilute in Ni, Si, Cu.
- Enrichment enhanced by low temperature.
- Cr switch-over at ≈680°C.

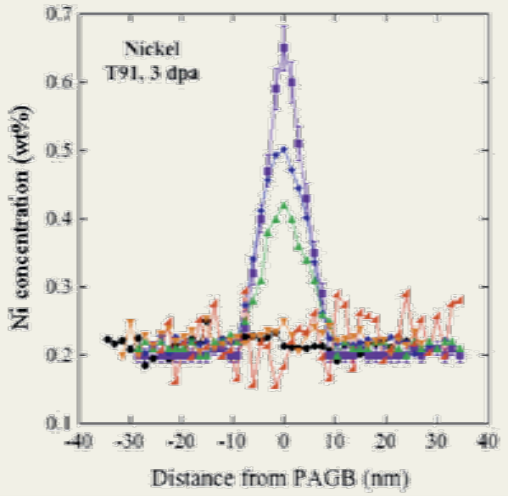

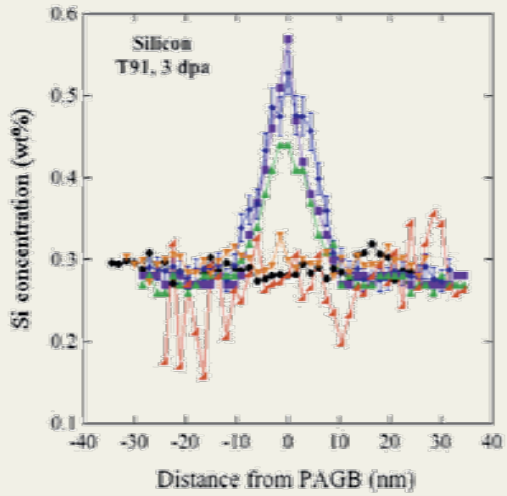

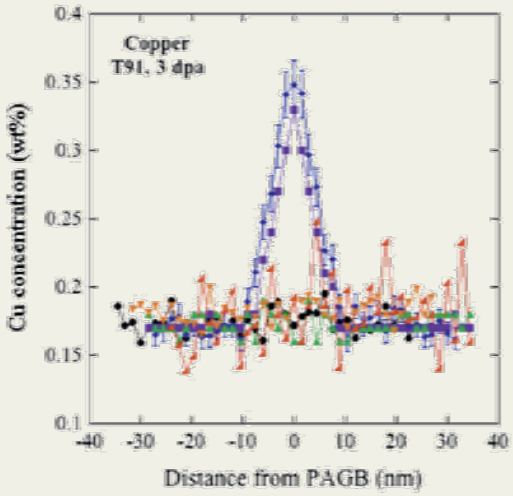

Radiation-induced segregation (RIS)

Enrichment/Depletion tendencies determined by solute-defect flux coupling!

$$J_i = -\sum_{j=1}^{N} L_{ij} \nabla \mu_j \qquad J_B = 0,\ J_V = J_I \ \text{(steady-state conditions)}$$

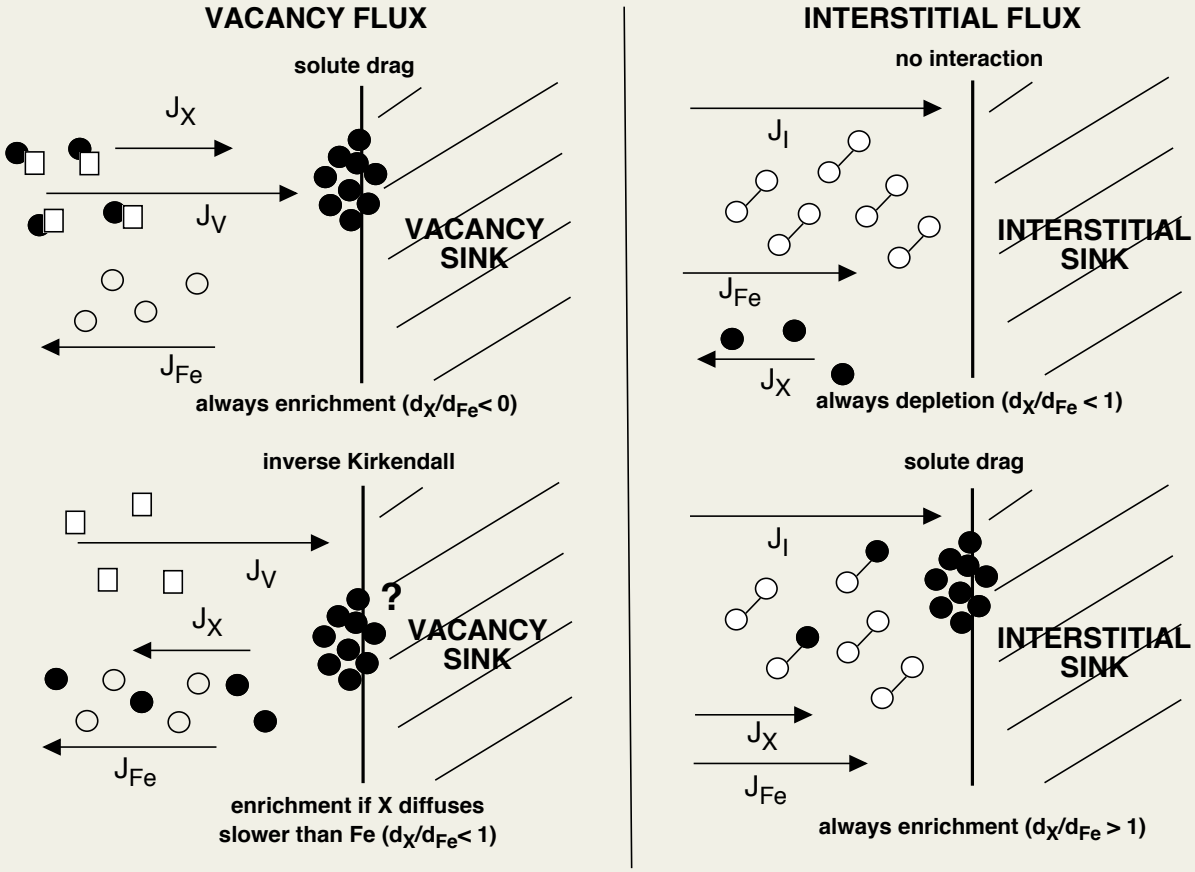

$$\frac{\nabla c_B}{\nabla c_V} = \frac{c_A c_B d_{AV} d_{AI}}{\left(c_B d_{BI} D_A + c_A d_{AI} D_B\right)} \left(\frac{d_{BV}}{d_{AV}} - \frac{d_{BI}}{d_{AI}} \right)$$

$$\frac{d_{BV}}{d_{AV}} = \frac{L^V_{AB} + L^V_{BB}}{c_B \left(L^V_{AA} + L^V_{AB} \right)}$$

$$\frac{d_{BI}}{d_{AI}} = \frac{L^I_{AB} + L^I_{BB}}{c_B \left(L^I_{AA} + L^I_{AB} \right)}$$

RIS tendencies

General trends:
- Enrichment at low T (vacancy drag).
- Fe(Cr) system very close to switch point at all T.

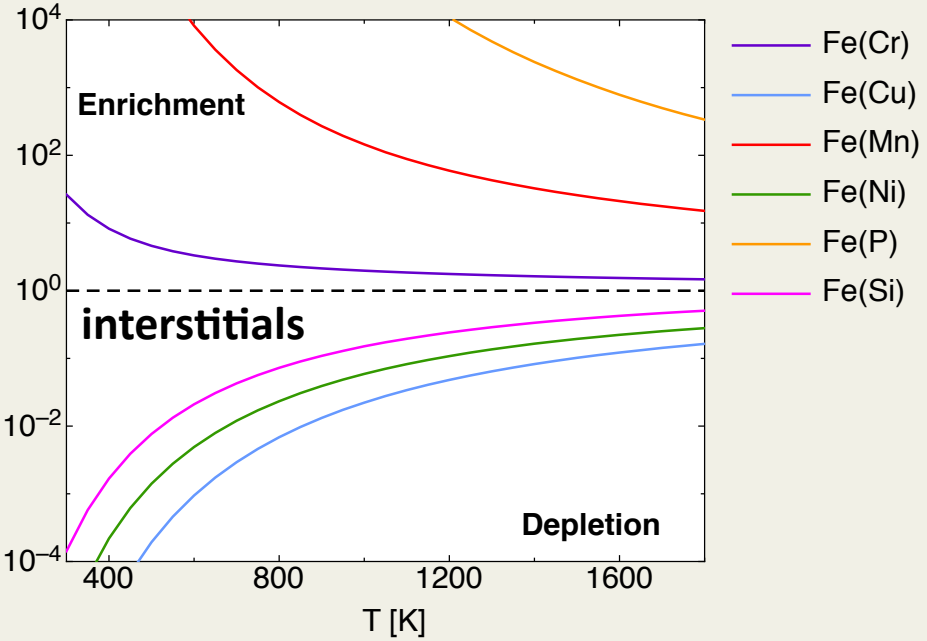

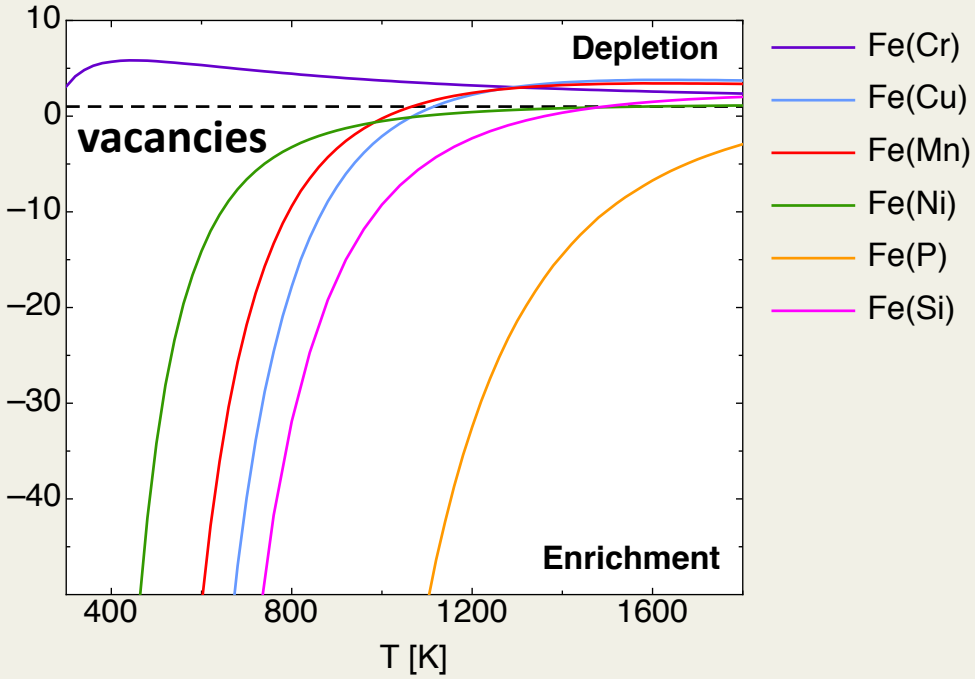

Summary by impurity

	Vacancy diffusion	Interstitial diffusion	Dominant mechanism*	RIS tendency
Cr	no drag	yes	in competition	V: Depletion I: Enrichment
Cu	drag T < 930 °C	no	vacancies	V: Enrichment I: Depletion
Mn	drag T < 825 °C	yes	interstitials	V: Enrichment I: Enrichment
Ni	drag T < 887 °C	no	vacancies (≈)	V: Enrichment I: Depletion
P	drag at any T	yes	interstitials	V: Enrichment I: Enrichment
Si	drag T < 1141 °C	no	vacancies (≈)	V: Enrichment I: Depletion

* Inferred by comparing magnitude of diffusion coefficient ratios d_{BV}/d_{AV} and d_{BI}/d_{AI}.

Conclusions

- Theoretical model to investigate and predict solute transport phenomena and solute-defect flux coupling, so to better understand diffusion processes leading to wanted or unwanted changes of local chemical composition in alloys.

- Very flexible and general method, applicable to many sorts of crystal structures and migrating objects (defect clusters, foreign interstitials, etc..).

- Exact transport coefficients are calculated through a mean field method by making use of accurate first principle calculations.

- Main findings
    a) Vacancy drag on all solutes but Cr, enhanced by low temperatures.
    b) Interstitial transport for Cr, P, Mn – not for Si, Cu, Ni.
    c) Vacancy-driven diffusion for Si, Cu, (Ni); interstitial-driven for P, Mn; both for Cr.
    d) Enrichment of solutes at grain boundaries and dislocations.

- Solid theoretical modelling of mechanisms for emrittling nanofeature formation in RPV steels.

Thanks for your attention!

Contact: messina@kth.se

Main reference: L. Messina *et al.*, PRB **90**, 104203 (2014).

ACKNOWLEDGMENTS

- P. Olsson, P. Efsing, Z. Chang (KTH)
- M. Nastar, F. Soisson, T. Garnier (CEA Saclay)
- C. Domain (EDF)
- L. Malerba (SKC-CEN)
- Financial support from Vattenfall and the Göran Gustafsson foundation